

Annihilation Fountain in the Galactic Center Region

C. D. Dermer & J. G. Skibo

E. O. Hulburt Center for Space Research, Code 7653,
Naval Research Laboratory, Washington, DC 20375-5352

ABSTRACT

Two different model-independent mapping techniques have been applied to *CGRO* OSSE, *SMM*, TGRS and balloon data and reveal a feature in the 0.511 MeV e^+e^- annihilation radiation pattern of our galaxy centered at $\ell \sim -2^\circ$ and $b \sim 10^\circ$ with a flux of $\sim 5 \cdot 10^{-4}$ 0.511 MeV ph $\text{cm}^{-2} \text{s}^{-1}$. If near the galactic center, then e^+ sources are producing $\sim 10^{42} e^+ \text{s}^{-1}$ which annihilate ≈ 1 -2 kpc above the galactic plane. A starburst episode within the inner few hundred pc of our galaxy would drive hot pair-laden gas into the halo, with the one-sidedness pointing to the site of initial pressure release at the onset of the starburst activity. Positrons lose energy and annihilate as they are convected upward with the gas flow, and we calculate high-latitude annihilation patterns and fluxes in accord with the observations. Changes in the ionization state when the escaping gas cools could give annihilation radiation substructure. The fountain of hot ($\sim 10^6$ - 10^7 K) gas rising into the galactic halo would be seen through its enhanced dispersion measure, thermal emission, and recombination radiation.

Subject headings: Gamma Rays: Theory — ISM: Supernova Remnants, Jets and Outflows — Nuclear Reactions, Nucleosynthesis, Abundances

1. Introduction

In addition to the previously identified (Purcell et al. 1993; Ramaty, Skibo & Lingenfelter 1994) 0.511 MeV annihilation glow from the disk and nuclear bulge of our galaxy, recent analyses (Purcell et al. 1997a, 1997b; Cheng et al. 1997) of data obtained with the Oriented Scintillation Spectrometer Experiment (OSSE) on the *Compton Gamma Ray Observatory*, the *Solar Maximum Mission*, the Transient Gamma Ray Spectrometer (Teegarden et al. 1996) on the *Wind* spacecraft, and GRIS, FIGARO, and HEXAGONE balloon experiments show a very significant annihilation emission component $\approx 5 \cdot 10^\circ$ north of the galactic plane in the general direction defined by the axis of the galactic center lobe (Pohl, Reich & Schlickeiser 1992). Imaging limitations of the γ -ray telescopes make it impossible to resolve fine structure, but the high latitude component appears extended rather than pointlike. If near the galactic center at distance $8d_8$ kpc, then e^+ sources are producing $\approx (2 - 3f/2)^{-1} 4 \cdot 10^{42} d_8^2 e^+ s^{-1}$ which annihilate ≈ 1 -2 kpc above the galactic plane. Here f is the fraction of e^+ which annihilate via positronium (Ps) formation.

Positron sources include radioactive emitters from supernovae and novae, black hole jets, and low-energy (≈ 10 -100 MeV nuc^{-1}) cosmic rays. Due to proximity to the galactic center and the feebleness of annihilation radiation from star-forming regions, we conclude that the region of enhanced e^+e^- annihilation radiation exists about 1 kpc above the galactic center. A starburst episode within the inner few hundred pc of our galaxy would drive hot pair-laden gas into the halo, with the one-sidedness pointing to the site of initial pressure release at the onset of the starburst activity. Here we investigate the production, transport, and annihilation of e^+ convected to high galactic latitudes in a wind produced in the galactic center region.

In Section 2, we consider e^+ production from supernovae, and summarize evidence for starburst activity in the galactic center region. A model for e^+ transport and annihilation in a fountain model is described in Section 3, and used to calculate a map of the annihilation emissivity from the direction of the galactic center. Predictions and a summary of the results are given in Section 4.

2. Positron Production from Supernovae and Galactic Center Activity

The origin of positrons through the decay of radioactive nuclei is confirmed by observations of ^{56}Co and ^{57}Co nuclear decay lines from SN 1987A (Matz et al. 1988; Kurfess et al. 1992), the ^{26}Al 1.809 MeV line found in clumped structure along the galactic plane (Diehl et al. 1995), and the ^{44}Ti nuclear decay line from Cas A (Iyudin et al. 1994). The mean lifetimes of the $^{56}\text{Ni} \rightarrow ^{56}\text{Co}$ and $^{56}\text{Co} \rightarrow ^{56}\text{Fe}$ decays in the $^{56}\text{Ni} \rightarrow ^{56}\text{Co} \rightarrow ^{56}\text{Fe}$ chain are 8.8 and 111.4 days, respectively, with a β^+ emitted 19% of the time in the latter reaction. Type Ia supernovae involving white dwarf detonation or deflagration produce a time-averaged e^+ production rate $\dot{N}_+^{56,\text{Ia}} \cong 1.4 \cdot 10^{43} \eta_{-2} M_{56} \dot{N}_{\text{Ia/C}}$ $e^+ s^{-1}$, where M_{56} is the average number of Solar masses of synthesized ^{56}Fe per SN Ia, $\dot{N}_{\text{Ia/C}}$ is the number of SN Ia per century throughout the Milky

Way, and $\eta = 10^{-2}\eta_{-2}$ is the escape fraction. Chan & Lingenfelter (1993) calculate the escape fraction to be in the range $0.1 \lesssim \eta_{-2} \lesssim 10$, and report (Woosley & Weaver 1992) that $0.6 < M_{56} < 0.9$. For core-collapse Type II supernovae, only an average $0.08M_{\odot}$ of ^{56}Fe is synthesized per SN, and the escape fraction could reach 0.7% for well-mixed ejecta, implying that $\dot{N}_{+}^{56,\text{II}} \cong 10^{42}\eta_{-2}(M_{56}/0.08)\dot{N}_{\text{II/C}} \text{ e}^{+} \text{ s}^{-1}$.

The mean lifetime of the $^{44}\text{Ti} \rightarrow ^{44}\text{Sc} \rightarrow ^{44}\text{Ca}$ chain is 78 yrs, with a positron produced 95% of the time in the latter decay. Compared to the mass of ^{56}Fe , a ^{44}Ti mass fraction $\zeta = 10^{-4}\zeta_{-4}$ in the range $0.3 \lesssim \zeta_{-4} \lesssim 1.4$ is calculated for SN Ia and $\zeta_{-4} < 25$ is found for SN II (Chan & Lingenfelter 1993). This gives $\dot{N}_{+}^{44} \cong 8 \times 10^{41}\zeta_{-4}M_{56}\dot{N}_{\text{SN/C}}$, noting that most e^{+} escape from the SN ejecta and mix with the surrounding medium. ^{26}Al decays into ^{26}Mg with a mean lifetime of 10^6 yrs, producing a positron 82% of the time. Production of ^{26}Al is most important in Type II SNe, though only $0.3 \cdot 10^{-5} \lesssim M_{26} \lesssim 20 \cdot 10^{-5}$ Solar masses of ^{26}Al are produced per SN II, depending on initial stellar mass and the treatment of semi-convection (Prantzos 1996). This gives $\dot{N}_{+}^{26,\text{II}} \cong 10^{41}(M_{26}/10^{-5})\dot{N}_{\text{II/C}} \text{ e}^{+} \text{ s}^{-1}$, a value probably insufficient to account for the $1.5 M_{\odot}$ of ^{26}Al required to explain the total observed (11) 1.809 MeV ^{26}Al line flux of $3.1(\pm 0.9) \cdot 10^{-4} \text{ cm}^{-2} \text{ s}^{-1}$ for which, at least, Wolf-Rayet stars and novae make important contributions.

An episode of starburst activity in a region a few hundred pc across enclosing the galactic center could account for Ginga observations (Koyama et al. 1989; Yamauchi et al. 1990) of 6.7 keV emission from He-like Fe at temperatures $\gg 10^7$ K. The hot gas in this scenario is produced by 10^3 SNe over the preceding 10^5 yrs, which would be mostly SNe II from massive star evolution unless the activity had persisted for a period much exceeding 10^5 yrs. Other indications (Hartmann 1995) of explosive events near the galactic center include large-scale X-ray structures, radio structures, and indeed the 1.809 MeV line. The radio emission of the galactic center lobe is explained by the synchrotron emission of nonthermal electrons convecting and diffusing outward (Pohl et al. 1992).

Within the limits of uncertainty, β^{+} production from SNe II could account for the flux of the high-latitude annihilation glow if $\dot{N}_{\text{SN/C}} \approx 1$ in the central 100-200 pc nuclear region of our galaxy and, furthermore, if e^{+} are transported to the annihilation site and efficiently annihilated. Pair-laden hot gas from the galactic center starburst would vent into the galactic halo while expanding, radiating and cooling, and slowing in transit from the galactic center to the lower-pressure galactic halo. While convecting outward, e^{+} would cool and annihilate with the plasma electrons in the hot wind, and this is our explanation for the observations (Purcell et al. 1997a, 1997b; Cheng et al. 1997). The venting would be preferentially one-sided due to the location of the initial starburst activity and the morphology of the confining gas.¹

¹We note that either Sgr A*, the putative $10^6 M_{\odot}$ black hole at the Galactic Center, or the less massive Einstein source (1E 1740.7-2428), weighing in at $\sim 10\text{-}10^2 M_{\odot}$, could produce a large enough e^{+} production rate if annihilation were efficient, but the origin of the elevated target region requires additional explanation.

3. Annihilation Fountain Model

We sketch a model for the fountain of rising annihilating gas energized by a starburst episode.² Suppose that gas rises with speed $10^7 v_7$ cm s⁻¹ from a region of radius $r_b = 100 r_{100}$ pc undergoing a starburst phase, implying a gas crossing time of order r_{100}/v_7 million years. We approximate the shape of the volume of the gas expanding into the galaxy’s halo by an inverted cone with opening angle χ , cut off at both ends, so that the cross sectional area of the fountain is $\pi r_b^2(1+u)^2$, where $u = z \tan \chi/r_b$ and z is the height above the galactic plane. Our major simplification, which can be relaxed in more general treatments, is that the gas rises with constant velocity. Continuity of the mass flux for a steady-state situation considered here (see Ramaty et al. 1992 for a treatment of time-dependent injection and annihilation in a uniform medium) implies that the density of the gas at the base of the fountain is $n_p^0 \cong 0.13 \dot{M}_{\odot/C}/(v_7 r_{100}^2)$ cm⁻³, where $\dot{M}_{\odot/C}$ Solar masses of gas are expelled per century from the starburst region and rise into the halo. The time- and spatially- averaged density distribution as a function of height z above the galactic plane is therefore $n_p(z) = n_p^0/(1+u)^2$.

The time scale for a positron injected with kinetic energy $m_e c^2(\gamma - 1)$ to thermalize with the background hot thermal gas is controlled primarily by Coulomb losses at mildly relativistic and nonrelativistic energies. Coulomb losses operate on a time scale of $\approx 0.5\beta(\gamma - 1)/(n_{-1}\Lambda_{30})$ million years, where Λ_{30} is the Coulomb logarithm divided by 30, the density is $0.1 n_{-1}$ protons cm⁻³, and βc is the positron’s speed. The kinetic energy distributions of positrons entering the ISM after SN II explosions are given for the ⁵⁶Co→⁵⁶Fe and the ⁴⁴Sc→⁴⁴Ca decays by functions peaking near 0.6 MeV with FWHM widths of ≈ 0.9 MeV and high-energy tails reaching to ≈ 1.45 MeV (Chan & Lingenfelter 1993). The fraction of e⁺ which annihilate in flight prior to thermalizing usually amounts to < 10% and these positrons do not contribute to the 0.511 line emission (Murphy, Dermer & Ramaty 1987). After entering the thermal pool, the positrons annihilate in a fully ionized thermal plasma through direct annihilation and radiative combination on a thermal annihilation time scale of $30/(\lambda_{-14} n_{-1})$ million years, where the annihilation rate coefficient $\lambda = 10^{-14} \lambda_{-14}$ cm³ s⁻¹ (Bussard, Ramaty & Drachman 1979). When a significant fraction of neutral atoms or partially ionized ions are present, the annihilation rate can dramatically increase because $\lambda_{-14} \rightarrow 10^6$ near temperatures of $\simeq 10^5$ K due to the onset of charge exchange processes which have atomic-sized cross sections. A pair of 0.511 MeV line γ rays comes from direct annihilation in the thermal gas and, one-quarter of the time, from annihilation via Ps formation.

We calculate the annihilation flux at height z after tracking the energy evolution and spatial propagation of the e⁺ following injection. The e⁺ height-dependent injection function is approximated by a Gaussian function which is allowed to be, in general, offset from the galactic plane. The FWHM width of the injection function is taken to be 180 pc, comparable to twice the scale height of massive stars. Though diffusion must be important for very relativistic e⁺ (Lerche

²The general picture also applies to plasma ejection from black hole jets.

& Schlickeiser 1980), we assume that the nonthermal and thermal e^+ are entrained in the hot gas and convect away from the galactic midplane with constant speed v_0 . The general e^+ equation of motion involves Coulomb, bremsstrahlung, adiabatic expansion, synchrotron and Compton energy losses, but for β^+ injection, only Coulomb and adiabatic expansion losses are important. The e^+ energy-loss rate from adiabatic expansion is given by $-\dot{\gamma}_{\text{adia}} = (4\gamma - 3 - \gamma^{-1})\dot{V}/(3V)$, which bridges the nonrelativistic and relativistic regimes and applies to high-beta plasmas, which is suitable for magnetic fields weaker than $\sim 10^{-3}$ Gauss. The volume expansion rate for the fountain geometry is $\dot{V}/V = 2v_0 \tan \chi / [r_b(1 + u)]$, from which we find that Coulomb losses dominate adiabatic expansion losses when $\beta(4\gamma - 3 - \gamma^{-1}) \lesssim K = 36\Lambda_{30}\dot{M}_{\odot/C}/[v_7^2 r_{100}(\tan \chi/0.1)]$.

After β^+ emission, positrons convect away from the galactic plane and, if injected with sufficiently low energies, thermalize with the background gas through Coulomb processes (excepting those few which annihilate in flight). We call the distance between injection and thermalization the Maxwell-Boltzmann length (MBL), which is a nonlinear function of the injection height z_i and the e^+ injection kinetic energy $m_e c^2(\gamma - 1)$. When Coulomb processes dominate, the MBL is given by $u_{\text{MB}} = [(1 + u_i)^{-1} - K_c^{-1}(\beta_i \gamma_i - \arccos \gamma_i^{-1})]^{-1} - 1$, where $u_{\text{MB}(i)} = z_{\text{MB}(i)} \tan \chi / r_b$. The constant $K_c = 2.4\dot{M}_{\odot/C}\Lambda_{30}/(v_7^2 r_{100} \tan \chi)$.

When $K \gg 1$, as with standard parameter values, positrons injected through β^+ production thermalize close to their injection site. Thus the spatial dependence of positrons thermalizing with hot gas is, in this regime, equal to the energy-integrated β^+ -injection function. Following thermalization, a positron continues to convect upward into the galactic halo until it either annihilates or merges with the dilute halo gas. The decay law through annihilation for the rising positrons is governed by the value of the temperature-dependent reaction rate coefficient $\lambda(T)$, the ionization state, composition, and density of the medium. For hot gases with $T \gtrsim 10^6$ K, the 2-photon direct annihilation channel is most important with $\lambda_{-14} \cong 1$. The decay law for thermal positrons annihilating in a thermal gas is $-\dot{N}_+(t) \cong N_+(t)\lambda n_p(t)$. From this equation, we derive the height-dependent differential production rate of 0.511 MeV annihilation line photons, given by

$$\dot{N}_{0.511 \text{ MeV}}(z) = \frac{2n_-^0 \lambda(T)}{(1 + u)^2 v_0} \int_0^z dz' \dot{N}_+^{\text{th}}(z') \exp[-K_a(\frac{1}{1 + u'} - \frac{1}{1 + u})]. \quad (1)$$

Here $\dot{N}_+^{\text{th}}(z)$ is the MB injection function differential in height z , which is obtained by convolving the β^+ injection function with its MBL and integrating over the initial energies of the β^+ positrons. The constant $K_a = 0.039\lambda_{-14}\dot{M}_{\odot/C}/(v_7^2 r_{100} \tan \chi)$, n_-^0 is the electron density at the base of the fountain, and $u^{(l)} = z^{(l)} \tan \chi / r_b$.

In the approximation where e^+ thermalize close to their injection site, equation (1) is easily solved to give the results shown in Fig. 1. The total e^+ injection rate is $10^{42}\dot{N}_{+42} e^+ \text{ s}^{-1}$ with $\dot{N}_{+42} = 1$. The solid curves give the integral 0.511 MeV photon production rate between the galactic midplane and height z , and the dashed curves give the differential 0.511 MeV production rate in units of $0.511 \text{ MeV ph s}^{-1} z(\text{pc})^{-1}$. The dotted curves represent the spatial e^+ distribution function, which are centered at and 50 pc above the galactic midplane in Figs. 1a and 1b,

respectively.

Before interpreting Fig. 1, note that $\dot{N}_{0.511 \text{ MeV}}(< \infty) \rightarrow 2 \cdot 10^{42} \text{ 0.511 MeV ph s}^{-1}$ if all e^+ annihilate. This limiting value is reached only if most β^+ injection occurs high above the galactic plane so that few e^+ are convected to negative values of z . Standard parameter assignment with no source offset and $\tan \chi = 0.1$ (Fig. 1a), corresponding to a 6° fountain opening angle, yields an integral annihilation flux of $\approx 3 \cdot 10^{41} \text{ 0.511 MeV ph s}^{-1}$, implying a one-sided annihilation efficiency of $\sim 15\%$. In contrast, when the fountain opens to 45° ($\tan \chi = 1$), the annihilation efficiency plummets because of the severe thinning of gas density with height. In Fig. 1b, the wind speed parameter for the hot gas is increased by an order of magnitude from the standard value and the injection Gaussian is offset by 50 pc. This also reduces the annihilation efficiency because flux continuity demands a reduced density in a steady-state approximation.

The overall shape of the differential 0.511 MeV production function is unusual in that it exhibits a broad plateau between $\approx 50 \text{ pc}$ and 1-2 kpc. Rather than decreasing monotonically with height above the galactic midplane, the maximum of the differential 0.511 MeV annihilation flux peaks downstream from the maximum of the Gaussian injection function. This can be understood by superposing contributions from discrete sources. The annihilation flux decreases downstream from a steadily emitting e^+ source as the radioactive debris convect outward with constant velocity. But the divergence of the wind vector at the galactic midplane means that the e^+ density at a height z_0 is proportional to the number of sources between the galactic midplane and z_0 . This quantity increases with height above the galactic midplane for reasonable injection distributions until the source injection function tails off. The underlying assumption of time- and spatial-averaging appears to be satisfied for our system, because $\sim 10^4$ SNe occur during the gas-crossing time scale of the starburst region. More detailed calculations must consider the spatial distribution and temporal evolution of the discrete SN events exploding throughout the region.

The rate at which 0.511 MeV annihilation photons are emitted between ≈ 0.1 and 2 kpc is $\cong 2 \cdot 10^{41} \dot{N}_{+42}$ and $\cong 3 \cdot 10^{41} \dot{N}_{+42} \text{ 0.511 MeV ph s}^{-1}$ for the top curves in Figs. 1a and 1b, respectively. To match the OSSE/*SMM*/TGRS/balloon data analyses (Purcell et al. 1997a, 1997b; Cheng et al. 1997) implies that annihilation occurs at the rate of $\approx 4 \cdot 10^{42} d_8^2 \text{ 0.511 MeV ph s}^{-1}$. Thus injection rates of $\dot{N}_{+42} \simeq 20$ and $\dot{N}_{+42} \simeq 13$ are required to match the observations for these two cases. Such rates could be supplied by β^+ production from freshly synthesized ^{44}Ti in SN II given the uncertainty of the ^{44}Ti mass fraction, the SNe rate, and the parameters of the outflowing wind. This rate could perhaps also derive from β^+ production in the $^{56}\text{Ni} \rightarrow ^{56}\text{Co} \rightarrow ^{56}\text{Fe}$ chain if either the calculated escape fraction or amount of synthesized ^{56}Ni per SN II were underestimated. Black hole e^+ production could provide an additional source of the positrons.

Fig. 2 shows a contour map of the annihilation flux produced by the galactic fountain, added to a disk and galactic bulge distributions fitted to the measured (Purcell et al. 1997a) annihilation emissivity. The axis of the fountain is directed away from the center of our galaxy along the

direction of the galactic center lobe, which is inclined in projection by $\sim 20^\circ$ from the axis of the North Galactic Pole. (Note that the location of the centroid of the spheroidal bulge flux is offset from the location of the galactic center.) The agreement of this idealized model with the data is satisfactory, and predicts that peak enhancement of the fountain’s annihilation flux occurs $\gtrsim 100$ pc above the galactic plane.

4. Predictions and Summary

Due in large part to gamma-ray observations with the OSSE instrument on *Compton*, a new component of the ISM has been discovered: hot plasma pushing into the galactic halo from a region of starburst activity surrounding the galactic center a few hundred pc in extent. The existence of the outflowing wind is suggested by radio and X-ray observations (Pohl et al. 1992; Koyama et al. 1989; Yamauchi et al. 1990; Morris & Serabyn 1996) and represents a low-power analog of nuclear starburst outflows detected in M82 and NGC 253 (Shopbell & Bland-Hawthorn 1997). Hot ionized plasma can be detected through pulsar dispersion measurements, and we predict a dispersion measure jump of ~ 50 when scanning across the fountain several degrees above the galactic plane. The difficulty is to have independent distance measurements of pulsars located > 8 kpc away. Continuum free-free and recombination $\text{Ly}\alpha$ lines of H, He, and Ps are predicted from the fountain, but obscuring foreground gas makes it difficult to view the galactic center region at optical and UV wavelengths. As ^{26}Al is convected upward with the flow, a characteristic decay law for the diffuse 1.809 MeV emission (Chen, Gehrels & Diehl 1995) should be observed, though at a flux level requiring at least *INTEGRAL* telescope sensitivities. Turbulent hot gas in the central region might also explain the broadened 1.809 MeV lines observed (Naya et al. 1996) with the GRIS instrument. The width of the 2γ 0.511 MeV line from annihilation in hot gas will be broader than the galactic disk 0.511 MeV line emission because of the larger temperature of the plasma, depending in detail on the dust content of the fountain, and the 3γ Ps continuum fraction f will be spatially varying (Ramaty, private communication).

If the annihilation fountain is our first clear view of a conduit of hot gas venting the starburst activity near the galactic center into the galactic halo, then it is likely that cosmic rays are efficiently transported into and diffuse throughout the halo along this route. The > 100 MeV EGRET (Hunter et al. 1997) and 408 MHz Effelsberg (Haslam et al. 1982) all-sky maps show enhanced emission north of the galactic plane which could be ascribed to this effect. Positrons which fail to annihilate in the fountain will diffuse throughout the halo and annihilate if they encounter the gaseous disk. This could explain the large scale height of the disk component of the diffuse annihilation radiation $\gtrsim 10\text{-}20^\circ$ away from the galactic center (Ramaty et al. 1994). Long-lived radioactivity produced by SNe would also trace this channel. Small-scale variations of the 0.511 MeV map would indicate localized OB associations, changes in the ionization state of the gas, and sites of black hole e^+ injection. More observations and analyses are required to understand better the activity occurring near the center of the Milky Way.

We thank members of the OSSE team, especially W. Purcell and J. Kurfess, for conversations about the annihilation radiation observations. We also acknowledge useful discussions with Drs. R. Ramaty, R. Schlickeiser, J. Lazio, and A. Harding. In addition, we acknowledge support from the Office of Naval Research.

REFERENCES

- Bussard, R. W., Ramaty, R., & Drachman, R. J. 1979, *ApJ*, 228, 928
- Chan, K. W. & Lingenfelter, R. E. 1993, *ApJ*, 405, 614
- Chen, W., Gehrels, N. & Diehl, R. 1995, *ApJ*, 440, L57
- Cheng, L. X. et al. 1997, *ApJ*, 481, L43
- Diehl, R. et al. 1995, *A&A*, 298, 445
- Hartmann, D. H. 1995, *ApJ*, 447, 646
- Haslam, C. G. T., Salter, C. J., Stoffel, H. & Wilson, W. E. 1982, *A&AS*, 47, 1
- Hunter, S. D. et al. 1997, *ApJ*, in press
- Iyudin, A. F. et al. 1994, *A&A*, 284, L1
- Koyama, K. et al. 1989, *Nature*, 339, 603
- Kurfess, J. D. et al. 1992, *ApJ*, 399, L17
- Lerche, I. & Schlickeiser, R. 1980, *ApJ*, 238, 1089
- Matz, S. et al. 1988, *Nature*, 331, 416
- Mezger, P. G., Duschl, W. J., & Zylka, R. 1996, *A&A*, 7, 289
- Morris, M. & Serabyn, E. 1996, *ARA&A*, 34, 645
- Murphy, R. J., Dermer, C. D., & Ramaty, R. 1987, *ApJS*, 63, 721
- Naya, J. et al. 1996, *Nature*, 384, 44
- Pohl, M., Reich, W., & Schlickeiser, R. 1992, *A&A*, 262, 441
- Prantzos, N. 1996, *A&AS*, 120, 303
- Purcell, W. R. et al. 1993, *ApJ*, 413, L85
- Purcell, W. R. et al. 1997a, *ApJ*, submitted
- Purcell, W. R. et al. 1997b, in *The Transparent Universe, Proceedings of the 2nd INTEGRAL Workshop, ESA SP-382*, in press
- Ramaty, R., Leventhal, M., Chan, K. W., & Lingenfelter, R. E. 1992, *ApJ*, 392, L63
- Ramaty, R., Skibo, J. G. & Lingenfelter, R. E. 1994, *ApJ*, 92, 393
- Shopbell, P. & Bland-Hawthorn, J. 1997, *ApJ*, submitted

Teegarden, B. J. et al. 1996, ApJ, 463, L75

Woosley, S. E. & Weaver, T. A. 1992, in Supernovae, ed. J. Audouze et al. (New York: Elsevier)

Yamauchi, S. et al. 1990, ApJ, 365, 532

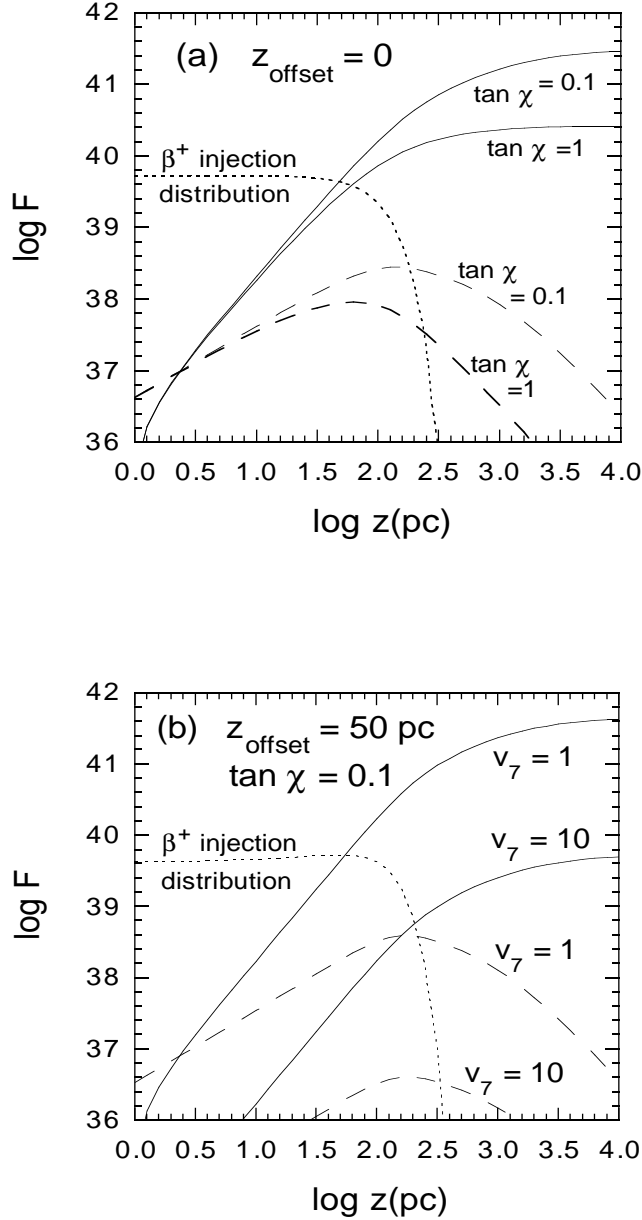


Fig. 1.— Height distribution of the differential (dashed curves) and integral (solid curves) 0.511 MeV annihilation emissivities produced in a fountain of hot gas rising upward with constant velocity v_0 . Except where noted, the opening angle of the fountain is $\chi = \arctan(0.1) = 5.^\circ 7$, $v_0 = 10^7 v_7 \text{ cm s}^{-1}$ with $v_7 = 1$, and the radius of the base of the fountain is 100 pc. We assume that 1 Solar mass of hot gas is ejected into the fountain per century. The dotted curves show the β^+ spatial injection function normalized to a total injection rate of $10^{42} \text{ e}^+ \text{ s}^{-1}$. Fig. 1(a) compares the effects of different opening angles χ for an injection function symmetric about the galactic midplane. Fig. 1(b) compares the effect of varying gas speeds for an injection function offset from the galactic midplane by 50 pc.

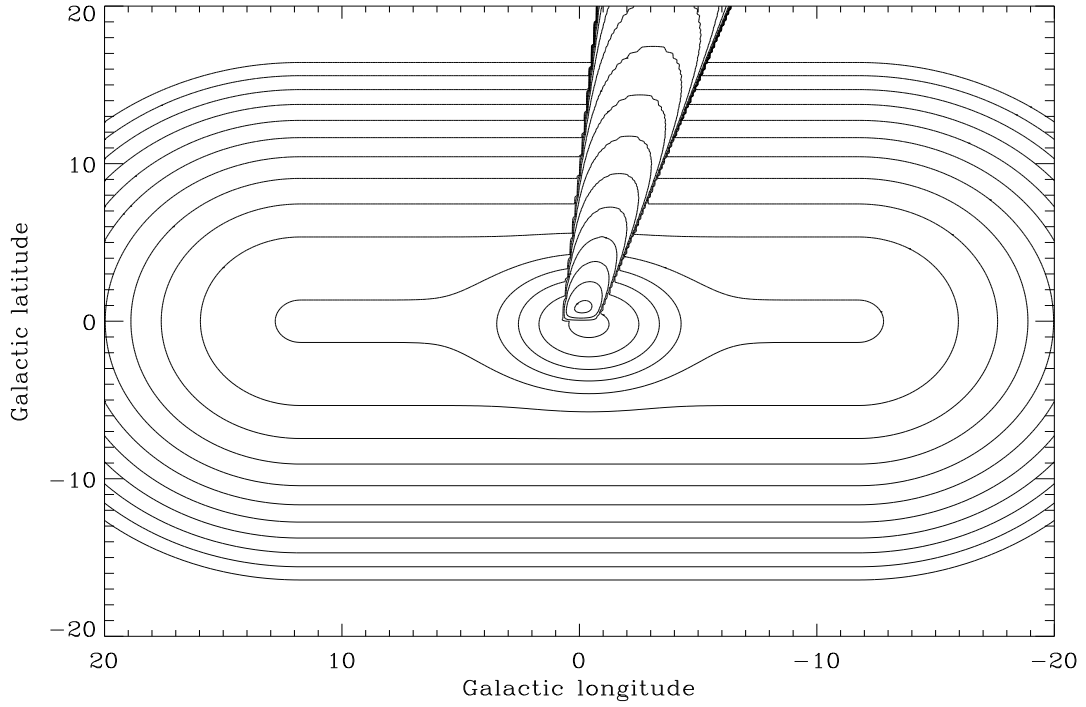


Fig. 2.— *Contour plot of the model annihilation emissivity of the Milky Way including the disk, galactic bulge, and fountain component. The contours are in units of $10^{-(2+n)/5}$ $0.511 \text{ MeV ph cm}^{-1} \text{ s}^{-1} \text{ sr}^{-1}$, with the central contour corresponding to $n = 1$.*